

Assessment of seismic performance of a Reinforced Earth wall using dynamic analysis



Ali Amini
Naesgaard Geotechnical Limited, North Vancouver, BC
Bill Brockbank
Reinforced Earth Company, Mississauga, Ontario
Ernest Naesgaard
Naesgaard Geotechnical Limited, Bowen Island, BC

ABSTRACT

A major project in the Greater Vancouver, BC, Canada, the Port Mann/Highway 1 project, is currently underway and includes construction of a new Port Mann Bridge over the Fraser River, widening Highway 1 for a distance of about 37 km and several mechanically stabilized earth (MSE) walls. The required seismic performance criteria for MSE walls were immediate functionality, repairable damage and no collapse after project design earthquakes with return periods of 475 yr, 975 yr and 2475 yr, respectively. To assess the seismic performance of a 12m high Reinforced Earth retaining wall on firm ground foundation, a series of two dimensional numerical dynamic analyses using the program FLAC were performed. The wall consisted of 16 layers of 9m long galvanized steel reinforcing strips at vertical spacing of 0.75m. The number of strips per metre length of the wall increased with depth. Numerical analyses indicated relative displacements within the reinforced earth structure in the range of less than 0.1m, 0.2m and 0.5m under 475 yr, 975 yr and 2475 yr design earthquakes, respectively. A number of strip layers yielded structurally, however the maximum calculated axial strains were less than 0.6%, 1.4% and 4.4% under 475 yr, 975 yr and 2475 yr design earthquakes, respectively and well below the allowable rupture strain.

RÉSUMÉ

Le grand projet « Port Mann/ Autoroute 1 » est actuellement en cours dans la région du Grand Vancouver en Colombie Britannique. Ce projet inclut la construction du nouveau pont Port Mann au dessus du fleuve Fraser, l'élargissement de l'Autoroute 1 sur une distance d'environ 37 km ainsi que plusieurs murs en terre mécaniquement stabilisée (TMS). Les critères d'exécution sismiques requis pour les murs TMS étaient : fonctionnalité immédiate, dommages réparables et aucun effondrement pour des tremblements de terre de conception avec des périodes de retour de 475 ans, 975 ans et 2475 ans, respectivement. Afin d'évaluer la performance sismique d'un mur de soutènement de Terre Armée de 12 m de hauteur et sur un sol de fondation ferme, une série d'analyses dynamiques numériques à deux dimensions a été effectuée. Le mur se composait de 16 couches d'inclusions métalliques de renforcement galvanisées de 9 m de long et avec un espacement vertical de 0.75m. Le nombre d'inclusions par mètre linéaire du mur augmentait avec la profondeur. Les analyses numériques ont montré des déplacements relatifs au sein de la structure en terre armée dans des limites de moins de 0.1m, 0.2m et 0.5m pour des tremblements de terre de conception de 475 ans, 975 ans et 2475 ans, respectivement. Un nombre de couches d'inclusions a atteint, structurellement, la limite d'élasticité, cependant les valeurs maximales calculées pour l'allongement axial étaient moins de 0.6%, 1.4% et 4.4% pour des tremblements de terre de conception de 475 ans, 975 ans et 2475 ans, respectivement et bien au-dessous de l'effort de rupture admissible.

1 INTRODUCTION

Reinforced Earth[®] structure consists of compacted granular soil, reinforced by steel strips which are connected to a segmental precast concrete facing. This composite structure forms a coherent mechanically stabilized earth (MSE) that is internally stable and can resist external loads.

The current Port Mann/Highway 1 project (PMH1) in Greater Vancouver, BC includes a new bridge over the Fraser River, 37 km of highway widening and MSE walls using a Reinforced Earth system. Throughout this paper the general term of MSE wall will be used.

Dynamic analyses were carried out to demonstrate that the proposed MSE walls were internally stable during seismic shaking and compliant with the seismic performance criteria of the project. The proposed MSE

walls had been designed according to an AASHTO based pseudo-static seismic design methodology.

Numerical analyses were performed for improved soft ground and firm ground foundation conditions with three suites of earthquake time histories with return periods of 475, 975, and 2475 years. This paper presents the methodology and results of a series of analyses for a 12 m high MSE wall resting on firm ground foundation.

2 PERFORMANCE OF REINFORCED EARTH STRUCTURES IN THE PAST EARTHQUAKES

Over the past forty years the MSE wall system under study has survived major earthquakes with no failures and little or no damage. These walls have undergone post earthquake inspections with the results duly recorded. Table 1 presents a summary of the survey of

Reinforced Earth structures after the Northridge, 1994 and Kobe, 1995 earthquakes. It is interesting to note that all the walls remained functional after the earthquakes even though measured or estimated ground accelerations exceeded design values. Some of the surveyed MSE walls were not even designed for seismic loading.

Figure 1 shows an MSE wall with minor damage adjacent to a collapsed bridge after the 1999 Izmit, Turkey earthquake. The MSE wall was a few metres from the fault rupture. The wall had been designed for a ground acceleration of 0.10 g as compared to the measured maximum horizontal ground acceleration of 0.4g.

Table 1. Summary of survey results on the Reinforced Earth structures after Northridge and Kobe earthquakes (adapted from Sankey and Segrestin, 2001)

Earthquake	Northridge 1994	Kobe 1995
Total walls surveyed	23	120
Wall Height > 5m	65%	70%
Wall Height > 10m	25%	15%
Actual PGA Measured/estimated	0.07-0.91g	0.27g
Design PGA	75% of cases less than actual PGA 50% of cases no seismic design	0.15-0.2g
Conditions after earthquake	All functional Minor spalling	All functional Minor cracking Some movements



Figure 1. Arifiye Reinforced, earth bridge approach MSE wall (Izmit earthquake, 1999), From SoilTech 2000

3 SEISMICITY OF THE REGION

The PMH1 project is located in south-western British Columbia which is an area with active seismicity. The major source of this seismic activity is the oceanic Juan de Fuca plate subducting under and compressing the continental North American plate. This results in three

potential earthquake sources: near-surface (0 to 30 km) crustal earthquakes, deep (40 to 50 km) intra-plate earthquakes within the subducting plate, and large inter-plate subduction earthquakes. The first two sources are accounted for in a probabilistic seismic model and are the predominant hazard for the site. The subduction earthquake is typically of larger magnitude but is at a significant distance (≈ 120 km) from the site and therefore, generally does not control the design.

Outcropping firm-ground response spectra for the 475-, 975- and 2475-year return period events, and for the deterministic subduction earthquake event are shown in Figure 2. Sets of out-cropping firm-ground earthquake records in two orthogonal directions were fitted to the design response spectra by others and provided for use in the design (Table 2).

4 SEISMIC PERFORMANCE CRITERIA

PMH1 project requires the MSE walls to be designed according to the following seismic performance criteria:

- 475 yr: Limited traffic access immediately after earthquake, restorable within days.
- 975 yr: Limited access to emergency traffic within days after earthquake and repairable for full function.
- 2475 yr: No collapse or loss of life.

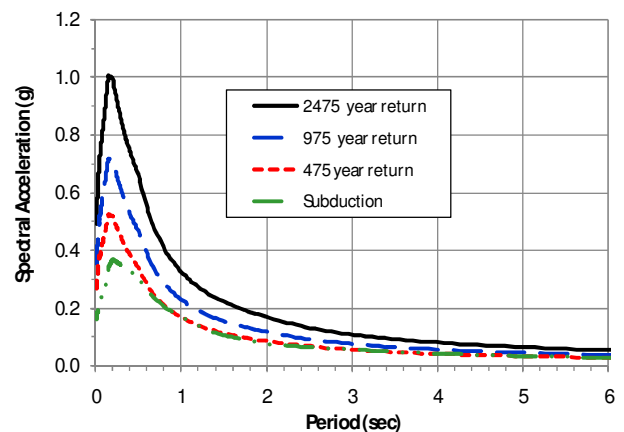


Figure 2. Firm ground (Class 'C' soil) outcropping design response spectra.

Table 2. Summary of PMH1 design ground motions

Earthquake Level	PGA (g)	Ground Motions
		Name, Year, Magnitude, Duration, Distance
475 yr	0.263	San Fernando, 1971, M6.6, 7s, 36.0 km Loma Prieta, 1989, M7.0, 20s, 9.7 km Olympia, 1949, M7.1, ~21s, 26.0 km
975 yr	0.355	Landers, 1992, M7.3, 31s, 13.7 km Loma Prieta, 1989, M7.0, ~20s, 9.7 km Chi Chi, 1999, M7.6, 32s, 7.1 km
2475 yr	0.494	Landers, 1992, M7.3, 31s, 13.7 km Loma Prieta, 1989, M7.0, ~20s, 9.7 km Chi Chi, 1999, M7.6, 32s, 7.1 km
Subduction	0.16	Mexico City, 1985, M8.1, 32s, 107 km

Dynamic numerical analyses were performed to get wall displacements and demands on the reinforcing strips for the purpose of assisting with assessment of compliance with the design criteria.

5 DYNAMIC NUMERICAL MODELLING

Two dimensional non-linear dynamic numerical analyses were carried out using the finite difference program FLAC version 6.0 (ITASCA, 2008).

5.1 Soil constitutive model

Mohr-Coulomb and UBCHYST constitutive models were used for the static and dynamic phases of analyses, respectively.

UBCHYST is developed at the University of British Columbia. It is a hyperbolic constitutive model with a Mohr Coulomb failure envelope and is used to simulate the non-linear hysteretic behaviour of soils during cyclic loading. The shear modulus is a function of stress ratio as presented in Equation [1] and Figure 3.

$$G_t = G_{\max} \cdot \left(1 - \frac{\eta_1}{\eta_f} \cdot R_f \right)^n \quad [1]$$

Where

G_t = tangent shear modulus

η = developed stress ratio = (τ_{xy} / σ'_v)

$\eta_1 = \eta - \eta_{\max}$ = change in stress ratio η since last reversal

η_{\max} = maximum η at last reversal

$\eta_{1f} = \eta_f - \eta_{\max}$ = change in η to reach failure envelope in direction of loading

$\eta_f = (\sin(\phi_f) + \text{Cohesion} \cdot \cos(\phi_f) / \sigma'_v)$

τ_{xy} = developed shear stress in horizontal plane

σ'_v = vertical effective stress

ϕ_f = peak friction angle

R_f and n = calibration parameters

UBCHYST was calibrated to reasonably match Seed and Idriss (1970) G/G_{\max} and Damping curves.

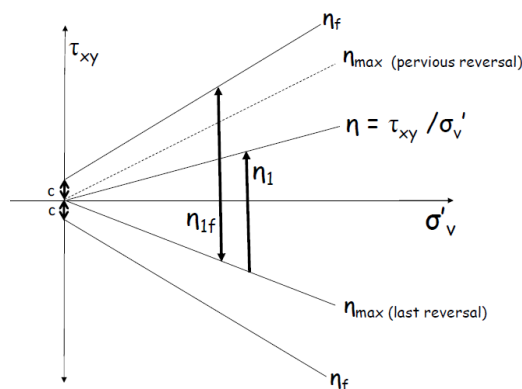


Figure 3. Failure envelope and parameters used in UBCHYST model

5.2 Geometry of the numerical model

The FLAC model was 12.75m high by 100m wide and consisted of 0.375m high by 0.4m wide elements in the proximity of wall. Elements became gradually wider towards the vertical boundaries of the model (Figure 4).

The model was constructed in 8 lifts, each including two rows of 9m long reinforcing steel strips and one concrete facing segment. The number of strips per metre of wall normal to the plane of analysis varied with depth as shown in Figure 4. FLAC built-in "strip" and "beam" elements were used to model reinforcing strips and facing segments, respectively. One end of strips was connected to their respective facing beams. Both ends of facing beams were pinned. The bottom of the facing wall was connected to its respective grid point.

The MSE fill and facing segments were separated using interface elements with a friction angle of 23 degrees.

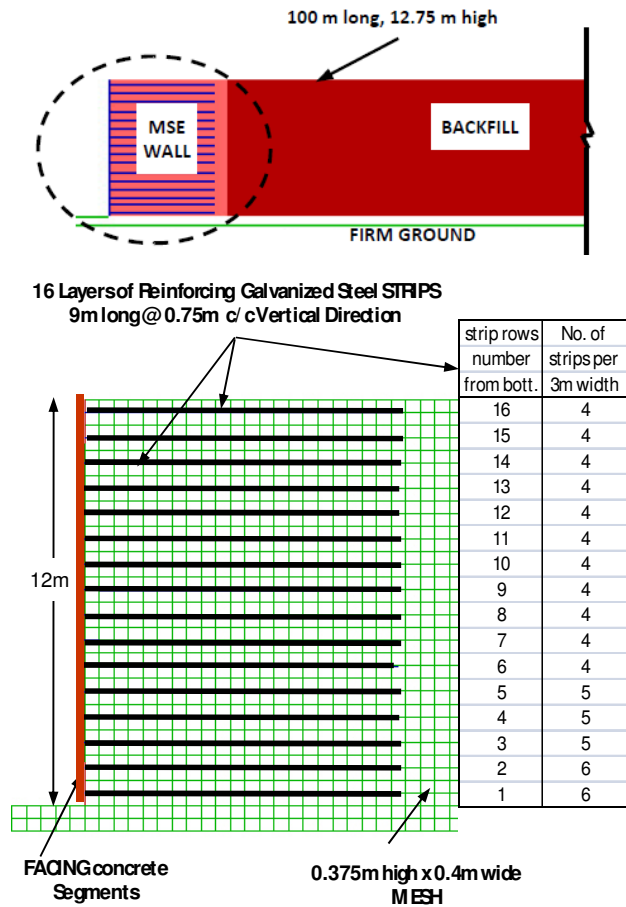


Figure 4. Geometry of the FLAC model

5.3 Soil conditions and material parameters

The case presented here includes granular fill for MSE volume and backfill overlying firm ground. Firm ground is defined as very dense soil with shear wave velocities between 360 and 760 m/s. Table 3 presents the assumed soil parameters.

5.4 Structural properties

Tables 4 presents the assumed properties for the reinforcing strips. The axial stiffness of the strips was calculated using the gross cross section area. The yield strength of the strips was calculated using a reduced cross section area assuming 100 year corrosion.

Table 5 presents the properties of the facing concrete segments. A reduced area was considered for the facing segments to account for reduction of overall axial stiffness due to inclusion of rubber pads between segments.

Table 3. Assumed soil properties in base case analyses

Soil Parameters	MSE Fill	Back fill	Firm ground
Unit weight (kN/m ³)	20	21	22
Peak Friction angle (deg)	34	36	N/A
Dilation angle (deg)	4	0	N/A
Cohesion	0	0	N/A
Poisson's ratio (-)	0.3	0.3	0.3
Shear modulus in static phase, G (MPa)	23	23	180
Shear wave velocity, V _s	Note 1	Note 1	400
Constitutive model in dynamic phase	UBCHYST	UBCHYST	ELASTIC
UBCHYST parameters, R _f , n	0.8, 2.5	0.8, 2.5	N/A

Note 1: Shear wave velocity was estimated according to Chillarige et al. (1997) correlation as follows:

$$V_s = (A - B \cdot e) \cdot \left(\frac{\sigma'_v}{P_a} \right)^n \cdot (K_o)^{0.125}$$

Where A=295, B=143 and n=0.26 for the Fraser River Sand. e is the void ratio assumed 0.68 equivalent to about 80% relative density.

Table 4. Assumed properties of reinforcing strips

Modulus of Elasticity (MPa)	2.1 x 10 ⁵
Poisson's ratio (-)	0.3
Gross cross section area (mm ²)	50 x 4 = 200
Corroded cross section area (mm ²)	50 x 2 = 100
Yield stress (MPa)	440
Yield strength (kN)	44
Rupture axial strain (-)	0.2
Allowable axial strain (-)	0.15
Initial apparent friction coefficient (-)	2
Minimum apparent friction coefficient (-)	0.67
Transition confining pressure (kPa)	120

Table 5. Assumed properties of facing concrete segments

Gross area (m ² /m)	0.14
Young's modulus, E (MPa)	2.5 x 10 ⁴
Moment of inertia, I (m ⁴ /m)	2.30 x 10 ⁻⁴
Density (kg/m ³)	2500
Modified area (m ² /m) (Note 1)	0.001

Note 1: Area reduced to account for reduction of overall axial stiffness due to inclusion of rubber pads between segments.

5.5 General procedure for numerical analysis

In FLAC, the dynamic analyses were carried out in the total stress mode in a chronological manner similar to the real conditions. The general procedure used for analyses included the following steps:

- Set up model grid and strip elements in 1.5m high lifts and bring to static equilibrium using Mohr-Coulomb models.
- Switch to UBCHYST constitutive model.
- Turn on dynamic configuration with large strain, and nominal 1% Rayleigh damping and bring to equilibrium by running with input motion of zero at bottom of the model and FLAC free field option at the side boundaries of the model.
- Set displacements to zero, apply the input time history of ground motions at base of FLAC model, and solve past end of earthquake shaking. Input ground motions were the with-in firm ground motions obtained by deconvolution of the design outcropping motions. Program SHAKE2000 was used for deconvolution. Figure 5 shows one of the design outcropping firm ground motions and its deconvoluted with-in motion at top of the firm ground.

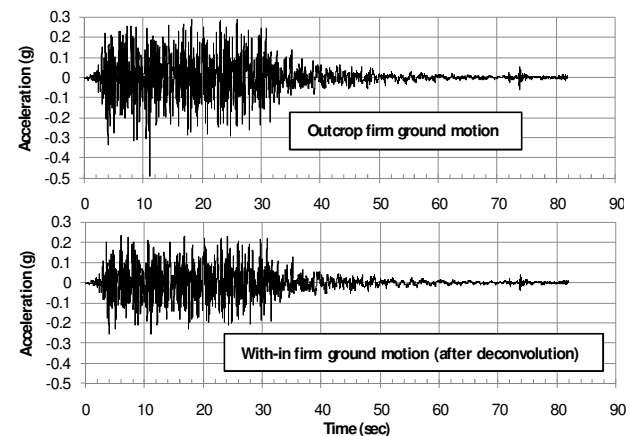


Figure 5. One of design firm ground motion time histories, CHICHI-NS-2475.

Top: Outcropping firm ground motion,

Bottom: With-in firm ground motion after deconvolution and a low pass filter of 15HZ

5.6 Numerical analysis results

Figure 6 shows the typical pattern of post-earthquake deformations of the wall. Note that the deformations are exaggerated for clarity. The deformation pattern suggests that the lateral displacement of the MSE wall is mainly due to shear deformation of soils between the reinforcing strips. In other words, the MSE wall can be assumed to be a shear beam with non-linear behaviour. Unbalanced mass results in biased lateral movements. In each cycle the wall moves out under the inertial load of MSE mass and the backfill. The inward movement of the wall is confronted with an additional resistance to drive the moving mass uphill similar to a passive condition. As a result, a net outward lateral displacement accumulates with each cycle and the system marches outward. As the wall moves out a depression zone develops behind the

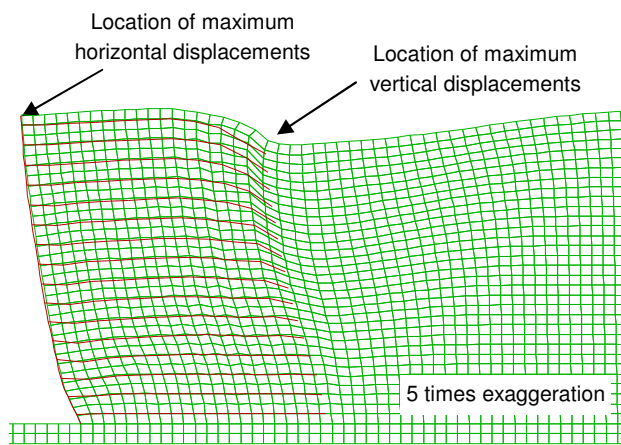


Figure 6 . Typical post-earthquake deformation pattern (CHICHI-NS-2475)- deformations are 5 times exaggerated.

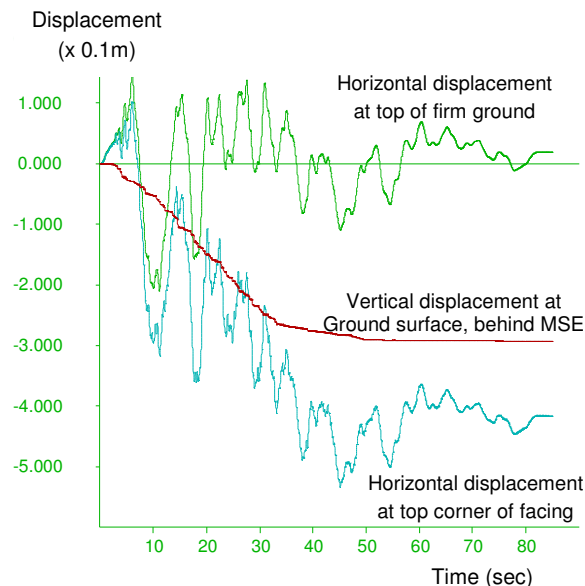


Figure 7. Time histories of maximum horizontal and vertical displacements during CHICHI-NS-2475

MSE volume. Maximum lateral and vertical displacements occurred at the top corner of the wall and behind the MSE volume, respectively. Figure 7 shows displacement time histories at these two locations for the most severe design earthquake (CHICHI-NS-2475). The input motion is also shown for comparison.

Unbalanced mass results in stress-strain curves with static shear stress bias. For example, In the middle of MSE wall where static shear stress bias was considerable, strains accumulated with each cycle (Figure 8-Top). On the other hand, static shear bias in the far field was relatively small and did not cause large accumulation of strains (Figure 8-Bottom). The shear stresses in Figure 8 are on horizontal and vertical planes. These shear stresses were used in the UBCHYST model for softening the shear modulus (Eq. 1). The maximum shear stresses occurred on other planes and were used to check the Mohr-Coulomb failure criterion.

Figure 9 presents a summary of calculated displacements under all design ground motions. Maximum horizontal and vertical displacements of about 0.45m and 0.3m, respectively were calculated. Displacements significantly decreased for 975 yr and 475 yr earthquakes.

Figure 10 shows the typical pattern of post-earthquake axial forces in the strips. Maximum axial forces occurred behind the facing and decreased gradually towards the back of the MSE wall as the loads were transferred to the ground through frictional resistance. The axial forces in the strips generally increased with depth and increased with time during earthquake shaking (Figure 10). Some of

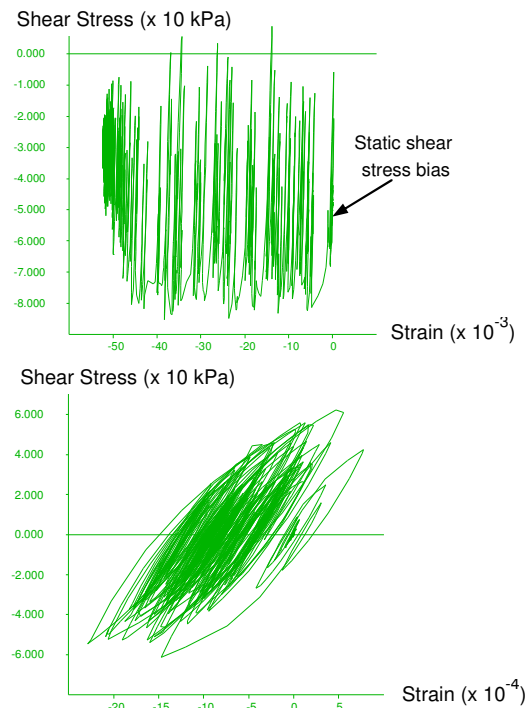


Figure 8. Typical stress vs strain curves during CHICHI-NS-2475, (Top) In the middle of MSE volume at 10.5m depth, (Bottom) In backfill at long distance from the MSE wall at 10.5m depth.

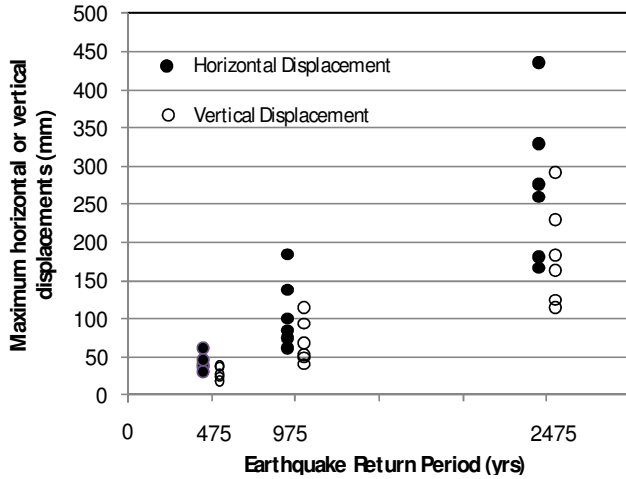


Figure 9. Summary of calculated maximum horizontal (at top corner of MSE wall) and maximum vertical displacements (behind MSE wall) under all design ground motions

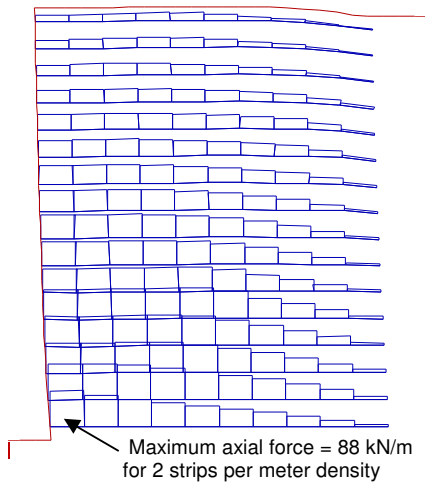


Figure 10. Typical distribution of axial forces in strips after CHICHI-NS-2475

the lower rows of strips reached their yield strength. For example in Figure 11, Row #2 had two strips per meter width of the wall and reached its yield strength of 88 kN/m at 5 seconds into the CHICHI-NS-2475 earthquake shaking. It may be argued that combination of the two extreme conditions, i.e. maximum corrosion and a seismic event, could be conservative.

Figure 12 presents a summary of the distribution of axial forces in the strips before and after earthquake shaking. Post-earthquake curves represent the average for 6 ground motions from each return period. The long term yield strength profile of strips (after 100 year corrosion) is also shown for comparison. All of the strips remained elastic in the static condition. The lower 6, 7 and 8 rows of the strips yielded in 475 yr, 975 yr and 2475 yr return period earthquakes, respectively.

Figure 13 shows accumulated axial strain in the strips at the end of the CHICHI-NS-2475 earthquake. Maximum axial strains in the range of 0.6%, 1.4% and 4.4% were

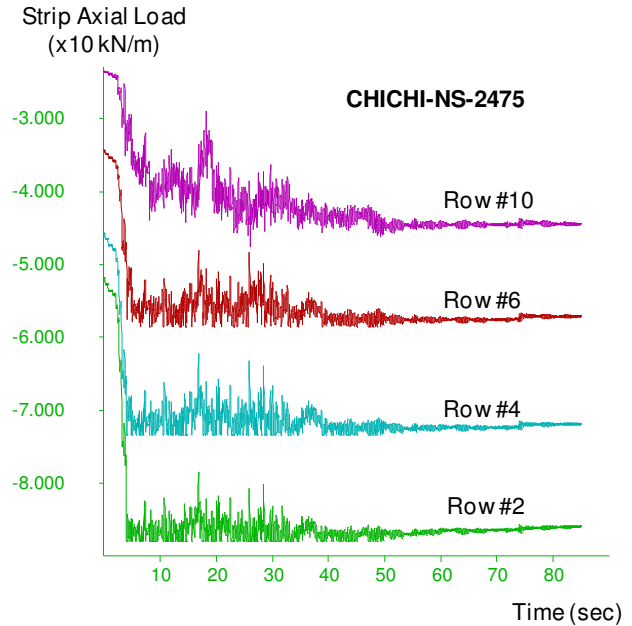


Figure 11. Time history of axial forces in strips immediately behind the facing under CHICHI-NS-2475. Strip row numbering is from bottom to top. Negative sign signifies tensile axial force.

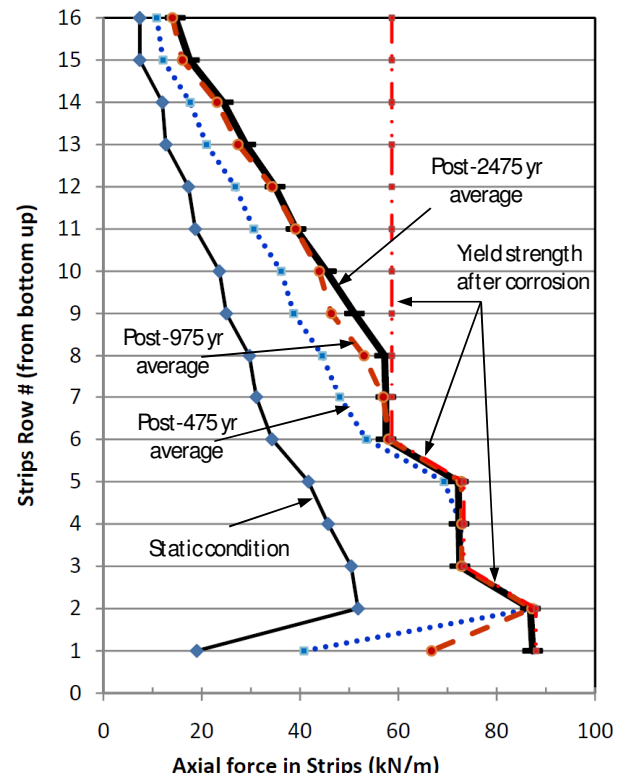


Figure 12. Comparison of axial forces in strips before and after earthquakes. Each post-earthquake curve represents the average of 6 ground motions.

calculated for 475 yr, 975 yr and 2475 yr return period earthquakes, respectively.

Figure 14 shows the time histories of lateral earth pressure at selected depths behind the facing and behind the MSE volume. The lateral pressure behind the facing increased during shaking and reached its maximum at the end of the shaking. On the other hand, the lateral pressure behind the MSE volume generally reduced with earthquake shaking.

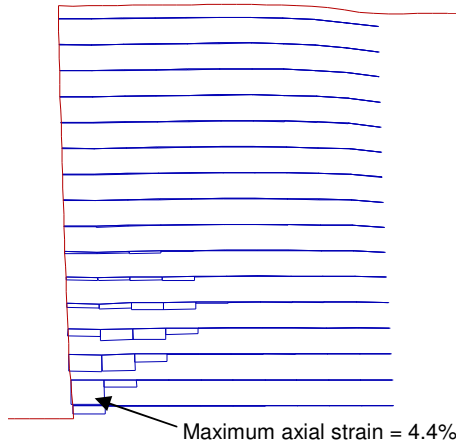


Figure 13. Distribution of axial strains in strips under CHICHI-NS-2475

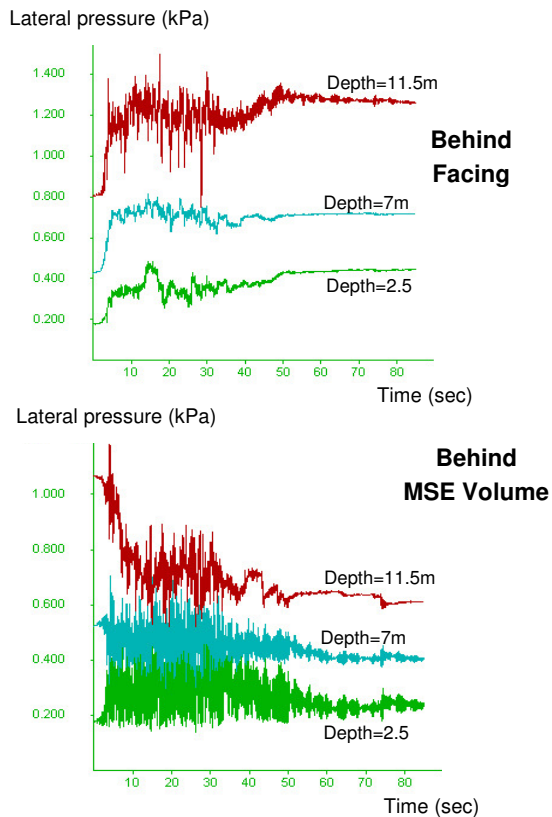


Figure 14. Time histories of lateral earth pressure (Top) Behind the facing, (Bottom) Behind the MSE volume

Figure 15-Top compares profiles of the coefficient of lateral earth pressure (K) before and after the CHICHI-NS-2475 earthquake behind the facing. The coefficient lateral earth pressure was calculated based on the post-earthquake lateral effective pressure obtained from the analyses divided by the initial vertical effective stress. The static K (before earthquake) was in the range of typical K_{Active} values. Earthquake shaking increased K to values greater than typical $K_{At-Rest}$ in the upper portion of the wall and to about $K_{At-Rest}$ in the lower portion of the wall.

Fig. 15-Bottom compares profiles of K behind the MSE volume. The static K was in the range of typical K_{Active} in the upper half and gradually increased to $K_{At-Rest}$ in the lower half. Earthquake shaking decreased the average value of K due to permanent lateral displacement of the MSE volume.

6 DISCUSSION

Numerical analysis provides much insight into behavioural patterns and modes of failure. However there is considerable uncertainty in the assumed parameters and analysis methodology, and seismic design in general. This should be understood and considered when using the results.

The calculated axial strains in the strips were well below the allowable rupture strains and are indicative of internal stability of the MSE wall.

A considerable scatter in the calculated displacement results was found among 975 yr and 2475 yr earthquake. This is partly due to the CHICHI ground motions being more severe than the other design motions. When considering the high return period and severity of earthquakes selected it is suggested that the use of the average calculated displacement rather than maximum displacement is appropriate for design. However, when considering uncertainties in earthquake motion, soil parameters, and the analyses methodology; the actual displacements could easily vary from 0.5 to 2 times the calculated values.

It should be noted that the calculated average displacements (especially for the 475 yr and 975 yr motions) are in the range of observed displacements of post-earthquake surveyed MSE walls. The relatively low calculated strains in the strips also agree with good past performance of MSE walls in earthquakes.

Initially the FLAC built-in hysteretic damping was tried in lieu of the UBCHYST constitutive model, however unreasonable results were obtained when there was a static bias (unreasonably small displacements and in some cases permanent displacements in a direction opposite the static bias) and therefore its use was discontinued.

7 SUMMARY AND CONCLUSIONS

A series of dynamic numerical analyses were carried out for a 12m high MSE wall with Reinforced Earth system founded on firm ground. The length and density of strips were determined using an AASHTO based pseudo-seismic design procedure. The main conclusions are:

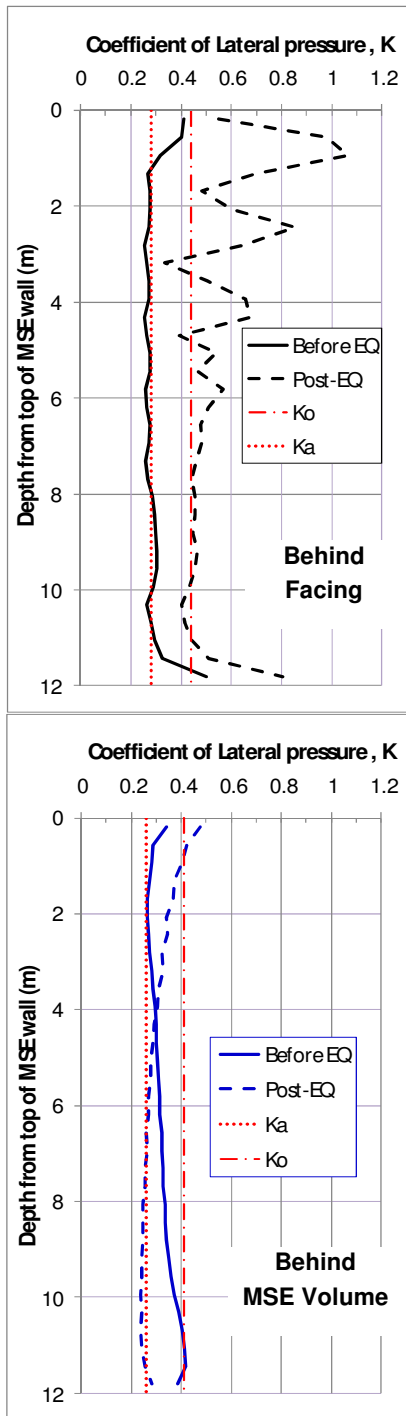


Figure 15. Comparison of the coefficient of lateral earth pressure before and after CHICHI-NS-2475 earthquake (Top) Behind the facing and (Bottom): Behind the MSE volume

K values were calculated as follows:

$K = \text{ratio of effective lateral stress to static effective vertical stress}$

$$K_{\text{Active}} = \frac{1 - \sin\phi}{1 + \sin\phi}$$

$$K_{\text{At-Rest}} = 1 - \sin\phi$$

- Numerical analyses indicated displacements in the range of less than 0.1m, 0.2m and 0.5m under 475 yr, 975 yr and 2475 yr design earthquakes, respectively. The average displacement of the six earthquake records at each return period were approximately half the above values.
- Some strips in the lower rows yielded structurally. However the maximum calculated axial strains were less than 0.6%, 1.4% and 4.4% under 475 yr, 975 yr and 2475 yr design earthquakes, respectively and well below the allowable rupture strain of 15%.

ACKNOWLEDGMENT

The writers would like to thank the Kiewit/Flatiron General Partnership for the opportunity to work on this project and acknowledge Kim Truong of The Reinforced Earth Company for her input in early FLAC analyses. We would also like to thank Professor Peter Byrne of the University of British Columbia for initial development of UBCHYST constitutive model.

REFERENCES

- ITASCA, 2008. "FLAC Version 6.0 Fast Lagrangian Analysis of Continua User's Manuals", Itasca Consulting Group Inc., Minneapolis Minnesota.
- SHAKE2000 (Ordonez 2007) . "SHAKE2000 - A computer program for the 1-D analysis of Geotechnical Earthquake Engineering Problems", Gustavo A. Ordonez, www.shake2000.com.
- Seed, H.B., and Idriss, I.M. 1970. Soil moduli and damping factors for dynamic response analyses. Report No. ERRC 70-10, Earthquake Engineering Research Center, University of California, Berkeley, California.
- Sankey, J.E. and Segrestin, P. 2001. Evaluation of Seismic Performance in Mechanically Stabilized Earth Structures ,Landmarks in Earth Reinforcements, Ochiai et al (eds), copywrite, 2001 Swets and Zeitlinger, ISBN 90 2651 863 3.
- SoilTech 2000. Performace of Reinforced Earth retaining walls near the epicentre of the Izmit earthquake. (Turkey, August 17, 1999). Pierre Segrestin, Internal Document of Freyssinet Technical Department, (SoilTech).